Scientia Iranica A (2019) 26(6), 3097–3108

SCIENTIA IRANICA

Sharif University of Technology
**Scientia Iranica**
*Transactions A: Civil Engineering*
http://scientiairanica.sharif.edu

# Seismic force modification factors for partitions in low-rise reinforced concrete buildings

**A.R. Kazerounian[a,*] and M.T. Kazemi[b]**

a. *Department of Civil Engineering, Sharif University of Technology, Kish Island, Iran.*
b. *Department of Civil Engineering, Sharif University of Technology, Tehran, Iran.*

Received 18 December 2016; received in revised form 28 October 2017; accepted 19 February 2018

**KEYWORDS**
Partition arrangement;
Out-of-plane;
Low-rise structures;
Modification factor;
Nonlinear seismic response history.

**Abstract.** Present codes of practice do not consider the effect of the arrangement of partitions in the plan of structure on the seismic demands of these non-structural components. In this paper, a modification factor has been proposed to modify provisions for those seismic demands. Seventy-two regular low-rise reinforced concrete moment frames, supporting some partitions, are exposed to seven appropriate ground motions. The nonlinear seismic response history analysis considering out-of-plane behavior of partitions was conducted using the OpenSees platform. The average values of peak responses from those earthquakes were obtained. The forces generated using the analytical method, some of which were verified by the existing study results, were compared with the values from the code, and a factor denoted by seismic force modification factor, $\Omega$, was proposed. A parametric study was carried out to study the effect of dominant parameters such as the arrangement of partitions, partition to structure height ratio, and length-to-height ratio of partitions on $\Omega$ values. For a majority of models, $\Omega$ values are larger for partitions that are located farther away from the center of the floor. Moreover, the modification factor could be as large as 1.85 for the partitions located on the middle floors.



## 1. Introduction

Non-Structural Components (NSCs) are those elements of a building that are not the integral portion of the main structure, but may be subjected to seismic excitation and, also, can have interaction with the supporting structure. Damage to NSCs may seriously impair a building's function and generate life hazard. The high percentage of the total cost of damage can relate to the failure in NSCs. To improve life safety and diminish the cost of loss, a better conception of structural and nonstructural subsystems is required. In various literature studies, acceleration induced in NSCs has been investigated by experimental and analytical methods with and without considering dynamic interaction between NSCs and primary (P) structures. In a study carried out by Marsantyo et al., Lepage et al., Sankaranarayanan and Medina, Sankaranarayanan, Aldeka et al., Aldeka et al., and Aldeka et al., new relations were recommended considering the parameters such as the position of the NSC in the main structure, service life of the component and building, damping ratio of the component and structure, extension of inelasticity of the structure, peak ground acceleration, NSC to P-structure height ratio, and P-structure eccentricity ratio [1-7]. Masonry infills are used in Reinforced Concrete (RC) frame structures as interior and exterior partition walls. In previous works, many researches have been carried out to investigate the effect of shear wall and masonry infill on the structures' behavior.

*. *Corresponding author.*
*E-mail addresses: kazerounian_sa@kish.sharif.edu (A.R. Kazerounian); kazemi@sharif.edu (M.T. Kazemi)*

doi: 10.24200/sci.2018.20201

The results showed that the infill walls increased the strength and stiffness of the structures [8-12]. Position and size of the openings in the infill wall are two major parameters that affect the behaviors of the infill walls and the frame. Tekeli and Aydin studied the seismic behavior of infilled RC frames with openings by the experimental method. Ten test specimens were constructed with a 1/3 scale and tested under cyclic lateral loading. The test results clearly show that the contribution of the infill wall to the behavior of RC frame has diminished significantly when the opening ratio is larger than 9% [13]. The arrangement of infill walls is also an important parameter that affects the seismic performance of the structure. Razzaghi and Javidnia studied the seismic performance of 18 models of the same structure, different arrangements of the infill walls, and four different ground motions using Perform 3D software. Results revealed that infill walls played a vital role in seismic performance of RC buildings. It was shown that noticeable changes might occur in seismic performance (e.g., experienced damage state, energy dissipation, etc.) of the same structure with different arrangements of the infill walls [14]. Out-Of-Plane (O.O.P) behavior and loading should be considered for stability of the wall under the seismic excitation. Mohammadi and Yasrebi investigated the O.O.P behaviors of walls and infills using rigid block concepts. It was shown that unreinforced walls of regular sizes (3 m high and 4.5 m long) were normally unstable under the strong earthquakes. In addition, supplying 3 reinforced bars at 1/4, 2/4, and 3/4 of the panel's height stabilizes the walls [15]. Preti et al. presented the results of an experimental campaign on the behavior of engineered masonry infill walls subjected to both in- and out-of-plane loading. Tests on two large-scale specimens and sub-assemblies were performed in order to evaluate the infill deformation capacity, the damage associated with different drift levels, and the mechanical properties of the components. A design method was developed for masonry infill walls capable of solving their vulnerability and detrimental interaction with the frame structure when subjected to seismic excitation [16].

The present codes of practice, such as ASCE 7-10 [17], do not consider the effect of parameters such as the arrangement of partitions in the plan of the P-structure on the seismic design force of partitions. It can be understood that if this effect is taken into account in the analysis of partitions, the generated force may be different considerably. Although some studies have been done to investigate the seismic forces in nonstructural element, no work has been reported to obtain the forces exerted on the partitions during earthquakes, considering O.O.P behavior, nonlinearity, and arrangement of partitions simultaneously. In this paper, considering the results of existing studies, the main objectives of the present research work are as follows:

- To obtain the O.O.P seismic design force by considering O.O.P behavior and nonlinearity of partitions;
- To compare analytical values of O.O.P seismic design forces with those given by ASCE 7-10 [17];
- To propose a factor in the modification of the seismic demands on partitions;
- To determine the effects of various parameters on O.O.P seismic design forces. The considered parameters include positions of partition in the plan of the supporting structure, partition to structure height ratio, and length-to-height ratio of partition.

Therefore, a study is undertaken involving the Finite Element (FE) analysis of the behavior of low-rise RC frame with hollow clay brick masonry infills. The forces perpendicular to partitions are defined through nonlinear seismic response history procedures. Analytical values of O.O.P seismic design forces are compared to ASCE 7-10 [17] for the seismic demands on NSCs. The factor of seismic force modification factor, $\Omega$, is considered to improve seismic demands on partitions given in ASCE 7-10 [17] provisions.

## 2. Methodology

It is required to model the structures properly with regard to the presence of partitions considering O.O.P and nonlinear behaviors. FE method is used to analyze a combined system that a partition forms with the structure to which it is attached. In this study, nonlinear seismic response history analyses have been conducted using the OpenSees platform in which the main structures and partitions are exposed to a set of seven ground motions. Standard 2800-14 [18] is used to scale the records; design of RC frames is based on ACI 318M-99 [19], and masonry infills are modeled using the method proposed by Kadysiewski and Mosalam [20]. The 3-story and 5-story models with partitions located in different positions were considered in this research. For any model, the average peak of O.O.P seismic design forces is obtained. The seismic forces of partitions are also calculated using ASCE 7-10 [17]. The analytical values of forces are divided by the values from the code; in addition, a factor, denoted by seismic force modification factor, $\Omega$, is determined.

### *2.1. Preliminary design of frames with a partition*

The structures are modeled, analyzed, and designed elastically in the first step. The stiffness effect of partitions is considered in this stage.

*2.1.1. Partition stiffness definition*
Partition stiffness is defined by FE method using ABAQUS software. The partitions are assumed to be made of hollow clay bricks with 190 mm × 180 mm × 90 mm dimensions. The plaster is used on the two faces of the partitions including gypsum and soil mortar and finish plaster. The followings properties are used for partition: thickness of partition, $t_p = 91$ mm; mass density, $\rho = 1529$ kg/m$^3$; compressive strength of the masonry unit, $f_m = 8.90$ MPa; expected compressive strength of masonry unit, $f_{me} = 1.30 f_m = 11.57$ MPa; masonry unit elastic modulus, $E_m = 550 f_{me} = 6.36$ GPa; and Poisson's ratio, $\upsilon_p = 0.15$.

In this study, three types of partitions are used according to different lengths, as shown in Table 1. The partition length is a clear length of the span measured between two columns. The clear height of all types of partitions is 2.88 m.

Following the elastic analysis, stiffness of partitions is calculated using the following equation:

$$K = \frac{F}{u}, \tag{1}$$

where $K$ is the partition stiffness, $F$ is the horizontal force obtained for the bottom surface of the partition, and $u$ is the horizontal displacement applied on the top surface of the partition. Values of partition stiffness are presented in Table 1.

For the preliminary analysis, the masonry partitions are modeled with equivalent diagonal struts and hinge ends in ETABS software. To affect the weight and stiffness of partitions in modeling, weight of partitions is applied to the lower beams, and the stiffness is considered based on the area of struts section by the following relationship:

$$A = \frac{KL}{E \cos^2 \theta}, \tag{2}$$

where $A$ is the area of two equivalent bracings, $K$ is the partitions stiffness obtained from Eq. (1), $L$ is the length of bracing, $E$ is the modulus of elasticity of bracings, considered as steel members ($E_s = 200$ GPa), and $\theta$ is the angle of bracing with respect to the horizon.

*2.1.2. Structural models*
After determining the area of equivalent struts, structures are initially modeled, analyzed, and designed by ETABS software according to the following specifications. A total of 72 regular structural models with 3 and 5 stories have been selected to carry out this study. The plan dimension of the structures with bay spans of 3 m, 4 m, and 5 m is 19 m × 19 m. Story height of the buildings is considered as 3 m. Figures 1 and 2 show 3D view and plan view of the buildings, respectively.

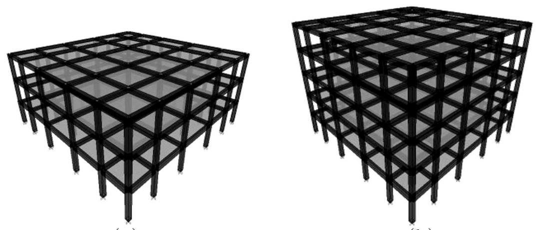


**Figure 1.** 3D view of structural models with (a) three and (b) five stories.

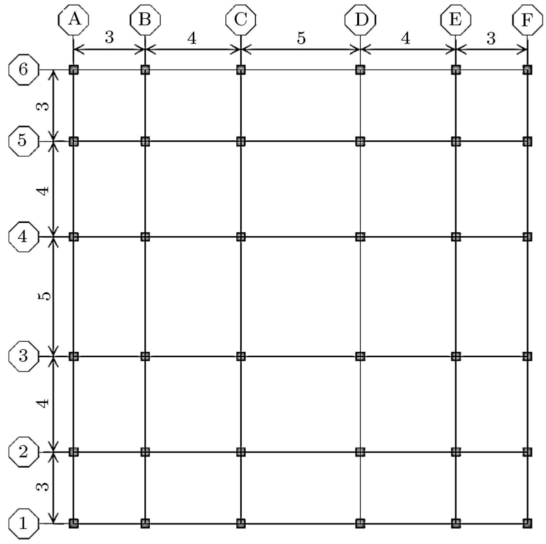


**Figure 2.** Plan view of the models (m).

According to Standard 2800-14 [18], the following properties have been provided to calculate earthquake load: response modification coefficient, $R = 5$; importance factor, $I = 1$; peak ground acceleration, $A = 0.35$; and site class = type II. Floors dead load is 1.90 kN/m$^2$, roof dead load is 2.93 kN/m$^2$, floors live load is 2.00 kN/m$^2$, and roof live load is 1.50 kN/m$^2$.

*2.1.3. Nomination rule*
A nomination rule for the classification of computation and data processing is required due to the large number of models. In this study, the models are named as

**Table 1.** Dimension and masses of partitions.

| Partition type | Span of bay (m) | Length (m) | Mass (kg) | Stiffness (MN/m) |
|---|---|---|---|---|
| Type A | 3.00 | 2.47 | 989.36 | 10.60 |
| Type B | 4.00 | 3.61 | 1447.34 | 24.50 |
| Type C | 5.00 | 4.56 | 1843.62 | 38.30 |

$S_iW_jF_kE_l$ where $i$ is the number of stories, $j$ is the length of span where the partition is located (m), $k$ is the level of floor where the partition is located, and $l$ is the distance between the partition and center of floor measured in the direction perpendicular to the partition (m).

According to the above nomination rule, the number of 3-story and 5-story models is 27 and 45, respectively.

### 2.2. The nonlinear analysis of frames with partition

The nonlinear seismic response history analysis is used with a 5% damping coefficient for the designed structures.

#### 2.2.1. Modeling of partition

Researchers have proposed various methods and codes to simulate the behavior of masonry walls. For example, Nwofor has introduced a modified stiffness matrix method for macro modeling of infilled RC frames [21]. In FEMA 356 [22], shear infill elements have been used for modeling masonry infill walls. The lateral rigidity of a masonry panel is considered by assuming a compression strut. Sabu and Pajgade carried out a seismic evaluation of existing RC buildings by simulating the action of infills similar to that of diagonal struts bracing the frame. The infills have been replaced by an equivalent strut proposed by Mainstone [23]. In addition, Kakaletsis proposed a continuous force-deformation model for masonry infill panels containing openings based on an equivalent strut method [24]. Mohebbi and Joghataei used the triple linear shear beam model to simulate the behavior of confined masonry wall under earthquake [25]. Eshghi and Sarrafi used an FE program, DIANA, for the FE modeling of fully grouted confined masonry walls, walls with unfilled head joints, two-story walls, walls with a lintel band, and walls with added vertical ties on the opening sides [26]. Furtado et al. modeled the masonry infill walls in RC buildings using OpenSees. Each infill panel is defined by considering four support strut elements with rigid in-plane behavior and a central element, where the in-plane nonlinear hysteretic behavior is concentrated. The forces developed in the central element are purely of tensile or compressive nature when submitted to in-plane solicitations [27].

In this paper, a macro modeling approach, called a single diagonal element, is adopted for partitions with regard to in-plane and O.O.P behavior interaction according to PEER 2008/102 [20].

#### 2.2.2. Data used in the analysis of models

In the modeling, the following material properties have been used for beams and columns.

*Beam and column*

To determine the specifications of concrete and steel, OpenSees manual is used [28]. Uniaxial materials Concrete 02 and Steel 02 (as provided in the OpenSees library) are used for concrete and steel, respectively. Shell and core concrete of sections are considered as unconfined and confined concretes, respectively. The stress-strain parameters required to define the confined concrete model in OpenSees are computed based on the study by Mander et al., which is capable of predicting the effect of confinement due to steel transverse reinforcement [29]. The material properties adopted for confined and unconfined concretes are shown in Table 2.

Representative plots for stress-strain behavior of confined and unconfined concretes are shown in Figure 3.

The parameters required to define the steel model in OpenSees are computed based on a study by Menegotto and Pinto [30]. The following are the material

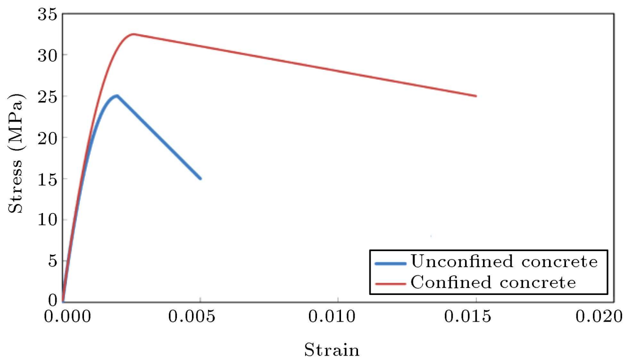


**Figure 3.** Stress-strain behavior of confined and unconfined concretes.

**Table 2.** Properties of concrete.

| | **Unconfined concrete** | **Confined concrete** |
|---|---|---|
| Compressive strength | $f'_c = -25$ MPa | $\boldsymbol{f'_{cc} = -32.5}$ **MPa** |
| Strain at compressive strength | $\varepsilon'_c = -0.002$ | $\boldsymbol{\varepsilon'_{cc} = -0.0026}$ |
| Ultimate strength | $f'_{cu} = -15$ MPa | $\boldsymbol{f'_{ccu} = -25}$ **MPa** |
| Strain at ultimate strength | $\varepsilon'_{cu} = -0.005$ | $\boldsymbol{\varepsilon'_{ccu} = -0.015}$ |
| Tensile strength | $f_t = -0.10 f'_c$ | $\boldsymbol{f_t = -0.10 f'_{cc}}$ |
| Tension softening stiffness | $E_{ts} = 0.20 f_t$ | $\boldsymbol{E_{ts} = 0.20 f_t}$ |

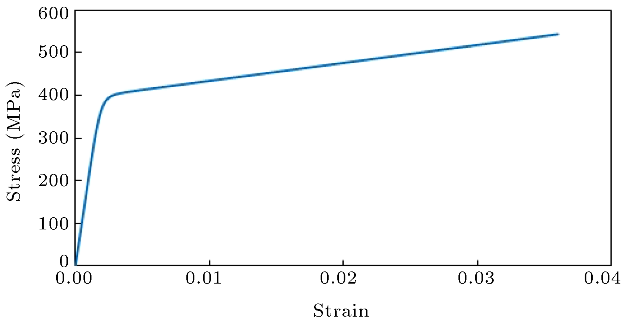


**Figure 4.** Stress-strain behavior of steel.

**Table 3.** Values of height ratio.

| Location of partition | $\alpha$ 3-story models | $\alpha$ 5-story models |
|---|---|---|
| 1st floor | 0.16 | 0.09 |
| 2nd floor | 0.50 | 0.30 |
| 3rd floor | 0.83 | 0.50 |
| 4th floor | – | 0.70 |
| 5th floor | – | 0.90 |

properties of steel adopted: yield strength, $F_y$ = 400 MPa; initial elastic tangent modulus, $E$ = 210 GPa; and strain hardening ratio, $b$ = 0.03. The representative plot for stress-strain behavior of steel is shown in Figure 4.

*Seismic loads*

The peak responses are obtained for seven considered earthquake ground motions, namely Parkfield (2004), Northridge (1994), San Fernando (1971), Loma Prieta (1989), Bam (2003), Manjil (1990), and Tabas (1978). The average values of peak responses from the considered earthquakes are also obtained; then, a parametric study is carried out. The accelerograms are scaled according to the Standard 2800-14 [18].

## 3. Parameters considered in this study

The main parameters that affect the seismic forces on the partitions are considered as follows:

(a) $\alpha = z/h$, partition to structure height ratio, where $z$ is the height of a structure of the center point of the partitions with respect to the base and $h$ is the average roof height of a structure with respect to the base. Values of $\alpha$ used in this study are presented in Table 3;

(b) $e = l/B$, distance to center index of partition, where $l$ is the distance between the partition and the center of floor in the direction perpendicular to the partition and $B$ is the floor dimension in that direction. Values of $e$ used in this study are presented in Table 4;

**Table 4.** Distance to center index of partition.

| Location of partition in axis | $e$ |
|---|---|
| Axis 1/6/A/F | 0.50 |
| Axis 2/5/B/E | 0.34 |
| Axis 3/4/C/D | 0.13 |

**Table 5.** Length-to-height ratio of partitions.

| Partition length (m) | $H$ |
|---|---|
| 2.60 | 0.86 |
| 3.60 | 1.25 |
| 4.60 | 1.58 |

(c) $H = L/D$, length-to-height ratio of partition, where $L$ and $D$ are length and height of partitions, respectively. Values of $H$ used in this study are presented in Table 5.

## 4. Determination of O.O.P seismic design forces of partitions

### 4.1. FE method

This study conducted the nonlinear seismic response history analysis using the OpenSees platform. Supporting structures and partitions were exposed to a set of seven ground motions. For any model and ground motion, the O.O.P seismic design force of partition was determined by FE analysis; then, this value was obtained based on the average of seven ground motion inputs. The O.O.P forces determined for all models are presented and shown in Tables A.1. and A.2. For example, the O.O.P seismic design force of the partition in model $S_3W_3F_1E_{2.5}$ comes out to be 9.53 kN.

*4.1.1. Verification of the models*

To verify the models, a numerical comparison is made between the forces obtained from this investigation with those from the approximate method proposed by Villaverde [31]. The proposed method is used to estimate the seismic response of nonlinear nonstructural components attached to nonlinear building structures in accordance with the following relationship:

$$F_p = \frac{C_p}{RR_p} S_a w_p, \tag{3}$$

where $S_a$ is the ordinate corresponding to the fundamental natural period and damping ratio of the structure in the acceleration response spectrum specified for the design of the structure, expressed as a fraction of the acceleration of gravity, $R$ and $R_p$ are strength reduction factors that account for the nonlinear behavior of the supporting structure and the nonstructural component, respectively, $w_p$ is the total weight of the nonstructural component, and $C_p$ is a component amplification factor calculated according to:

$$C_p = \frac{1}{\sqrt{\frac{2w_p}{W} + \frac{(1+0.5T)^2-1}{200\Phi_0^2}}} \leq \frac{\sqrt{200\Phi_0}}{1+0.5T}, \tag{4}$$

where $W$ is the total weight of the building, $T$ is the fundamental natural period of the structure, and $\Phi_0$ is calculated according to:

$$\Phi_0 = \frac{Wh_{av}}{\sum_{i=1}^{N} W_i h_i}, \tag{5}$$

where $W_i$ and $h_i$ respectively denote the weight and elevation above the ground of the building's $i$th floor, $h_{av}$ is the average of the elevations above the ground of the points of the building to which the nonstructural component is connected, and $N$ denotes the number of floors in the building.

The following are the values adopted in the calculations of O.O.P seismic design forces of partitions using Eq. (3): $S_a = 1.85$, $R = 5$, and $R_p = 2.50$.

The models considered for verification are 3-story structures with partitions located in three different span bays on the middle floor. The structures have the least distance to the center index of the partition, because the approximate method proposed is not a factor that corresponds to the effect of a nonstructural position in the plan. Properties of models are almost the same in the present and previous studies. It makes highly realistic data for the verification. The estimated seismic forces and those obtained from FE analysis are presented in Table 6.

Figure 5 indicates a comparison between the forces obtained by FE analysis with those by the approximate method proposed by Villaverde [31]. The amount of O.O.P seismic design forces of the partitions obtained using OpenSees is, on average, 10% greater than the values estimated by the approximate method. This difference results from the lack of consideration of the distance between the partition and the center of the plan in the approximate method. The reasonable agreement between both forces can be clearly seen in the whole length-to-height ratio, thus further facilitating the validation of the FE model used in this study.

**Table 6.** Comparison of the O.O.P seismic design forces.

| **Models** | $C_p$ | $F_p$ **(kN) [31]** | $F_p$ **(kN) (FE) (Present study)** |
|---|---|---|---|
| $S_3W_3F_2E_{2.5}$ | 7.97 | 11.45 | 12.60 |
| $S_3W_4F_2E_{2.5}$ | 7.94 | 16.69 | 18.34 |
| $S_3W_5F_2E_{2.5}$ | 7.33 | 19.62 | 21.66 |

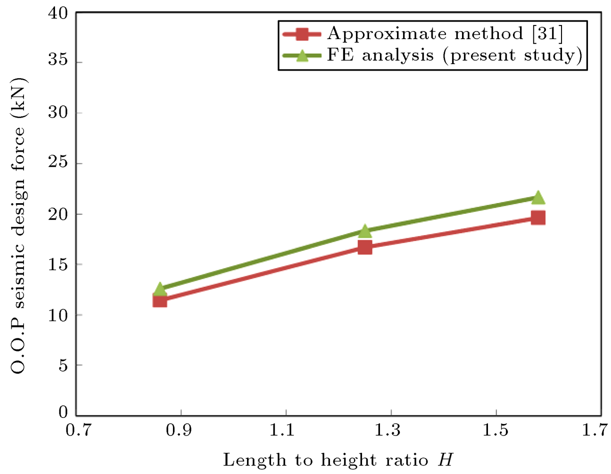


**Figure 5.** O.O.P seismic design force for partitions by FE analysis and the approximate method.

### 4.2. *ASCE 7-10 provisions for seismic demands on non-structural components [17]*

In ASCE 7-10 [17], the horizontal seismic design force, $F_p$, is applied at the component's center of gravity and distributed relative to the component's mass distribution and is determined by:

$$F_p = \frac{0.40 a_p S_{DS} W_p}{\frac{R_p}{I_p}} \left(1 + 2\frac{z}{h}\right), \tag{6}$$

where $z$ is the height in structure of point of attachment of component with respect to the base, $h$ is the average roof height of structure with respect to the base, $S_{DS}$ is the spectral acceleration in short period, $a_p$ is the component amplification factor, $I_p$ is the component importance factor, $W_p$ is the component operating weight, and $R_p$ is the component response modification factor. Minimum of $F_p$ is $0.30 S_{DS} I_p W_p$ which needs not to be more than $1.60 S_{DS} I_p W_p$.

#### *4.2.1. seismic design forces of partitions*

By using ASCE 7-10 [17] procedure, the seismic demands on partitions are determined. The following are the values adopted in the calculations: $S_{DS} = 1.85$, $a_p = 1$, $I_p = 1$, and $R_p = 2.50$. According to the above values, the O.O.P seismic design forces of partitions are estimated and listed for 3-story and 5-story models in Tables A.1. and A.2., respectively. For example, the O.O.P seismic design force of the partition in model $S_3W_3F_1E_{2.5}$ reached 6.57 kN.

## 5. Seismic force modification factor

The O.O.P seismic design forces of partitions obtained from FE analyses are smaller or greater than those calculated using Eq. (6). Following the previous comparison, a factor denoted by the seismic force modification factor, $\Omega$, is introduced to quantify the effect of parameters on the seismic design forces and is equated as in the following:

$$\Omega = \frac{F_n}{F_A}, \tag{7}$$

where $F_n$ is the O.O.P seismic design force defined based on the FEM solution, and $F_A$ is the O.O.P seismic design force defined based on ASCE 7-10 [17].

Seismic force modification factor is employed to evaluate the effect of various parameters on the seismic design forces perpendicular to the partition computed by the relationship in ASCE 7-10 [17]. This proposed factor has the potential to modify seismic demands on partitions defined by the code. Hence, the O.O.P seismic design forces of partitions could be attained by multiplying those obtained from the code by the seismic force modification factor, $\Omega$, without the need for the analytical method.

### 5.1. Computational results

The factor, $\Omega$, estimated for 3-story and 5-story models using Eq. (7) is given in Tables A.1. and A.2., respectively. For example, this factor for model $S_3W_3F_1E_{2.5}$ reaches 6.57 kN. Representative plots for $\Omega$ versus partition to structure height ratios are shown in Figures 6 and 7 for models with partitions of different lengths and positions in the plan.

It can be observed that the seismic force modification factor is larger for the partitions located on the middle floors. This is due to Eq. (6) of ASCE 7-10 [17], which is based on the equivalent static method and only a linear relationship between O.O.P force of partition and the ratio of the floor to roof elevations from the building grade. Moreover, the effect of the interaction between structure and partition is neglected in that relationship. ASCE 7-10 [17] provisions are almost appropriate for partitions mounted on the upper and lower floors, unlike middle floors. The factor, $\Omega$, can address both an increase and a decrease in seismic demands on partitions' values due to the changing position of partitions in the supporting structure. In other words, the arrangement of partition in the plan of the structure changes the values of O.O.P seismic design forces. The length-to-height ratio of partition also affects $\Omega$ values.

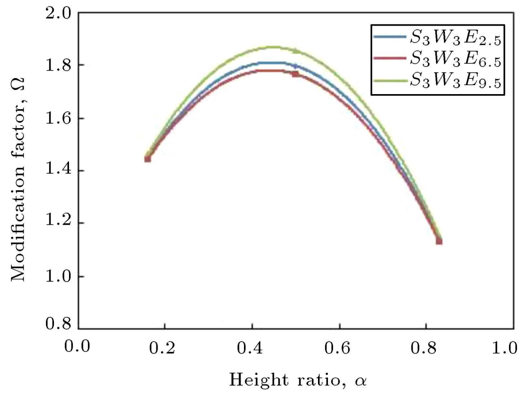


(a) Models $S_3W_3E_l$ with $H = 0.86$

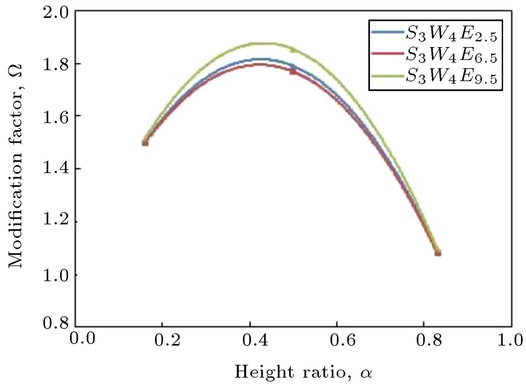


(b) Models $S_3W_4E_l$ with $H = 1.25$

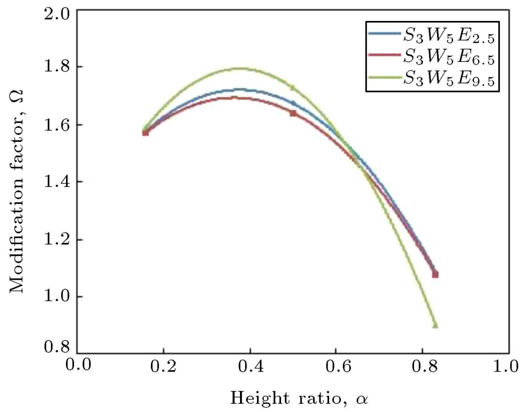


(c) Models $S_3W_5E_l$ with $H = 1.58$

**Figure 6.** Seismic force modification factor of 3-story models for various height ratios.

## 6. Summary and conclusions

This study proposed a seismic force modification factor, $\Omega$, and evaluated the dependence of the proposed factor on various parameters and characteristics (i.e., the distance to center index of partition in the plan of the supporting structure, partition to structure height ratio, and length-to-height ratio of partition). This proposed factor has the potential to modify the seismic demands on partitions defined by ASCE 7-10 [17], which means the O.O.P seismic design forces of partitions. The advantage of using factor $\Omega$ is that it can address both the increase and decrease of values of seismic demands of partitions due to the changing position of partitions in the structure. The results of the study demonstrate that the amplification of the partitions seismic demands can occur in different height ratios of the partition. Several conclusions can be drawn based on the forces obtained by the numerical

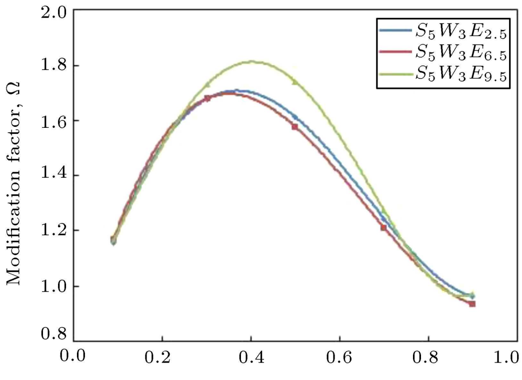


(a) Models $S_3W_3E_l$ with $H = 0.86$

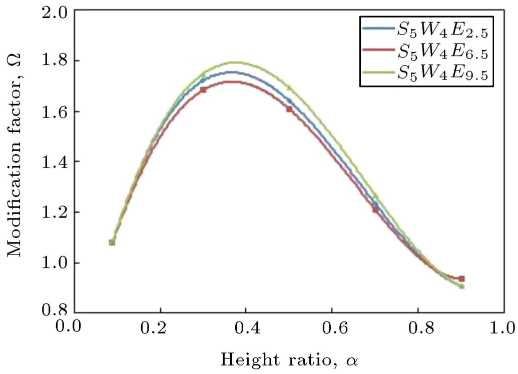


(b) Models $S_5W_4E_l$ with $H = 1.25$

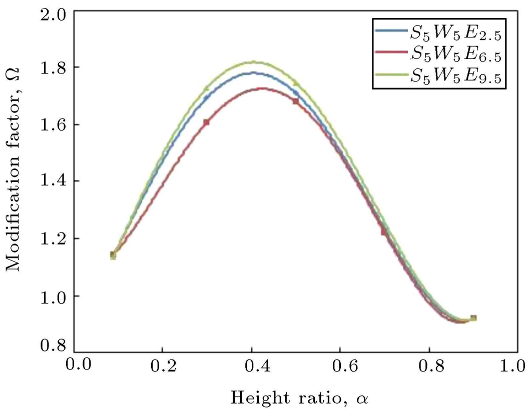


(c) Models $S_5W_5E_l$ with $H = 1.58$

**Figure 7.** Seismic force modification factor of 5-story models for various height ratios.

analysis compared to the values estimated based on ASCE 7-10 [17] provisions for seismic demands on non-structural components. The most important ones are listed below:

- The seismic force modification factor could be as large as 1.85;
- $\Omega$ values are higher for the partitions located on the middle floors;
- In most models, $\Omega$ values are maximum for partitions located farther away from the center of the floor. Therefore, code provisions are of low accuracy in calculating seismic design force on partitions mounted on the building facades;
- The length-to-height ratio of the partition adversely affects $\Omega$ values for most 3-story models. The obtained results show that $\Omega$ values increase as the length of partition decreases;
- For the partitions mounted on the first floor, $\Omega$ values are almost identical for all the cases with the same length-to-height ratio of partition and the number of stories;
- The seismic force modification factors are significantly affected by the partition to structure height ratio.

## Nomenclature

| | |
|---|---|
| $A$ | Area of two equivalent bracings (Eq. (2)) |
| $A$ | Peak ground acceleration (g) |
| $a_p$ | Component amplification factor (Eq. (6)) |
| $B$ | Floor dimension in the direction perpendicular to the partition |
| $l$ | Distance between partition and center of floor in the direction perpendicular to the partition in determination $e$ |
| $b$ | Strain hardening ratio of steel |
| $C_p$ | Component amplification factor (Eq. (3)) |
| $D$ | Height of partition |
| $E$ | Young's modulus of elasticity of bracings (Eq. (2)) |
| $e$ | Distance to center index |
| $E_m$ | Masonry elastic modulus |
| $E_{ts}$ | Tension softening stiffness of concrete in Table 2 |
| $F$ | Horizontal force generated on the upper surface of the partition (Eq. (1)) |
| $F_A$ | Out-of-plane seismic design force defined based on ASCE 7-10 (Eq. (7)) |
| $f'_c$ | Compressive strength of unconfined concrete in Table 2 |
| $f'_{cc}$ | Compressive strength of confined concrete in Table 2 |
| $f'_{ccu}$ | Ultimate strength of confined concrete in Table 2 |
| $f'_{cu}$ | Ultimate strength of unconfined concrete in Table 2 |

| | |
|---|---|
| $f_m$ | Compressive strength of the masonry |
| $f_{me}$ | Masonry expected compressive strength |
| $F_n$ | Out-of-plane seismic design force defined based on the numerical solution (Eq. (7)) |
| $F_p$ | Horizontal seismic design force (Eqs. (3) and (6)) |
| $f_t$ | Tensile strength of concrete in Table 2 |
| $F_y$ | Yield strength of steel |
| $H$ | Length-to-height ratio |
| $h$ | Average roof height of structure with respect to the base (Eq. (6)) |
| $h_{av}$ | Average of the elevations above the ground of the points of the building to which the nonstructural component is connected (Eq. (5)) |
| $h_i$ | Elevation above the ground of the building's floor (Eq. (5)) |
| $I$ | Seismic importance factor |
| $I_p$ | Component importance factor (Eq. (6)) |
| $K$ | Partition stiffness (Eqs. (1) and (2)) |
| $L$ | Length of bracing (Eq. (2)) |
| $L$ | Length of partition in determination $H$ |
| $R$ | Response modification coefficient (Eq. (3)) |
| $R_p$ | Component response modification factor (Eqs. (3) and (6)) |
| $S_a$ | Ordinate corresponding to the fundamental natural period and damping ratio of the structure in the acceleration response spectrum (Eq. (3)) |
| $S_{DS}$ | Spectral acceleration in short period (Eq. (6)) |
| $T$ | Fundamental natural period of the structure (Eq. (4)) |
| $t_p$ | Thickness of partition |
| $U$ | Horizontal displacement applied on the upper surface of the partition (Eq. (1)) |
| $W$ | Total weight of the building (Eq. (4)) |
| $W_i$ | Weight above ground of the building's $i$th floor (Eq. (5)) |
| $W_p$ | Component operating weight (Eqs. (3) and (6)) |
| $z$ | Height in structure of the center point of the partition with respect to the base (Eq. (6)) |
| $\alpha$ | Partition to structure height ratio |
| $\varepsilon'_c$ | Strain at compressive strength of unconfined concrete in Table 2 |
| $\varepsilon'_{cc}$ | Strain at compressive strength of confined concrete in Table 2 |
| $\varepsilon'_{ccu}$ | Strain at ultimate strength of confined concrete in Table 2 |
| $\varepsilon'_{cu}$ | Strain at ultimate strength of unconfined concrete in Table 2 |
| $\zeta$ | Damping ratio |
| $\theta$ | Angle of bracing with respect to the horizon (Eq. (2)) |
| $\upsilon_p$ | Poisson's ratio of partition |
| $\rho$ | Mass density of partition |
| $\Phi_0$ | Amplitude in a mode shape of the structure when this mode shape has been normalized so as to attain a unit participation factor (Eq. (4)) |
| $\Omega$ | Seismic force modification factor (Eq. (7)) |

## References


1. Marsantyo, R., Shimazu, T., and Araki, H. "Dynamic response of nonstructural systems mounted on floors of buildings", *12th World Conference on Earthquake Engineering*, Auckland, New Zealand (2000).

2. Lepage, A., Shoemaker, J.M., and Memari, A.M. "Accelerations of nonstructural components during nonlinear seismic response of multistory structures", *Journal of Architectural Engineering*, ASCE, **18**, pp. 285-297 (2012).

3. Sankaranarayanan, R. and Medina, R.A. "Acceleration response modification factors for nonstructural components attached to inelastic moment-resisting frame structures", *Earthquake Engineering and Structural Dynamics*, **36**, pp. 2189-2210 (2007).

4. Sankaranarayanan, R. "Seismic response of acceleration-sensitive nonstructural components mounted on moment-resisting frame structures", Ph.D. Dissertation, Maryland University, College Park (2007).

5. Aldeka, A., Chan, A.H.C., and Dirar, S. "Effects of torsion on the behavior of non-structural components mounted on irregular reinforced concrete multi-story buildings", *4th ECCOMAS Thematic Conference on Computational Methods in Structural Dynamics and Earthquake Engineering*, Kos Island, Greece (2013).

6. Aldeka, A.B., Chan, A.H.C., and Dirar, S. "Response of non-structural components mounted on irregular RC buildings: comparison between FE and EC8 predictions", *International Journal of Earthquakes and Structures*, **6**(4), pp. 351-373 (2014).

7. Aldeka, A., Dirar, S., Chan, A.H.C., and Martinez-Vazquez, P. "Seismic response of non-structural components attached to reinforced concrete structures with different eccentricity ratios", *International Journal of Earthquakes and Structures*, **8**(5), pp. 1069-1089 (2015).

8. Govalkar, V., Salunke, P.J., and Gore, N.G. "Analysis of bare frame and infilled frame with different position of shear wall", *International Journal of Recent Technology and Engineering*, **3**(3), pp. 67-72 (2014).

9. Mahmud, K., Islam, M.R., and Al-Amin, M. "Study the reinforced concrete frame with brick masonry infill due to lateral loads", *International Journal of Civil and Environmental Engineering,* **10**(4), pp. 35-40 (2010).

10. Shaharban, P.S. and Manju, P.M. "Behavior of reinforced concrete frame with in-fill walls under seismic loads using etabs", *International Journal of Civil Engineering and Technology*, **5**(12), pp. 181-187 (2014).

11. Niruba, S., Boobalakrishnan, K.V., and Gopalakrishnan, K.M. "Analysis of masonry infill in a multistoried building", *International Refereed Journal of Engineering and Science*, **3**(3), pp. 26-31 (2014).

12. Agrawal, N., Kulkarni, P.B., and Raut, P. "Analysis of masonry infilled RC frame with and without opening including soft story by using equivalent diagonal strut method", *International Journal of Scientific and Research Publications*, **3**(9), pp. 1-8 (2013).

13. Tekeli, H. and Aydin, A. "An experimental study on the seismic behavior of infilled RC frames with opening", *Scientia Iranica*, **24**(5), pp. 2271-2282 (2017).

14. Razzaghi, M.S. and Javidnia, M. "Evaluation of the effect of infill walls on seismic performance of RC dual frames", *Int. J. Adv. Struct. Eng.*, **7**, pp. 49-54 (2015).

15. Mohammadi, Gh.M. and Yasrebi, F. "Out of plane behavior of walls using rigid block concepts", *International Journal of Structural Engineering and Mechanics*, **34**(3), pp. 335-350 (2010).

16. Preti, M., Migliorati, L., and Giuriani, E. "Experimental testing of engineered masonry infill walls for post-earthquake structural damage control", *Bull. Earthquake Eng.*, **13**, pp. 2029-2049 (2015).

17. ASCE/SEI 7-10, *Minimum Design Loads for Buildings and Other Structures*, American Society of Civil Engineers, Reston, VA, USA (2010).

18. Building & Housing Research Center, *Iranian Code of Practice for Seismic Resistant Design of Buildings*, Standard No. 2800-14, 4th Edn., BHRC publication, Tehran, Iran (2014).

19. ACI 318M-99, *Building Code Requirements for Structural Concrete*, American Concrete Institute, USA (1999).

20. Kadysiewski, S. and Mosalam, K.M. "Modelling of unreinforced masonry infill walls considering in-plane and out of plane interaction", Pacific Earthquake Engineering Research Center, Report No. 2008/102, College of Engineering, University of California, Berkeley, California, U.S. (2009).

21. Nwofor, T.C. "Modified stiffness matrix method for macro-modelling of infilled reinforced concrete frames", *International Journal of Civil and Environmental Engineering*, **12**(2), pp. 53-73 (2012).

22. FEMA-356, *Prestandard and Commentary for the Seismic Rehabilitation of Buildings*, Building Seismic Safety Council, Washington D.C., USA (2000).

23. Sabu, D.J. and Pajgade, P.S. "Seismic evaluation of existing reinforced concrete building", *International Journal of Scientific and Engineering Research*, **3**(6), pp. 1-8 (2012).

24. Kakaletsis, D. "Analytical modelling of masonry infills with openings", *International Journal of Structural Engineering and Mechanics*, **31**(4) (2009).

25. Mohebbi, M. and Joghataei, A. "Optimal TMDs for improving the seismic performance of historical buildings", *International Journal of Science and Technology, Scientia Iranica*, **23**(1), pp. 79-90 (2016).

26. Eshghi, S. and Sarrafi, B. "Effect of openings on lateral stiffness and strength of confined masonry walls", *International Journal of Science and Technology, Scientia Iranica*, **21**(3), pp. 457-468 (2014).

27. Furtado, A., Rodrigues, H., and Arede, A. "Modelling of masonry infill walls participation in the seismic behavior of RC buildings using OpenSees", *Int. J. Adv. Struct. Eng.*, **7**, pp. 117-127 (2015).

28. Mazzoni, S., McKenna, F., Scott, M.H., Fenves, G.L., et al., *Open System for Earthquake Engineering Simulation, OpenSees Command Language Manual* (2006).

29. Mander, J., Priestley, M., and Park, R. "Theoretical stress-strain model for confined concrete", *Journal of Structural Engineering*, ASCE, **114**(8), pp. 1804-1826 (1988).

30. Menegotto, M. and Pinto, P.E. "Method of analysis for cyclically loaded RC plane frame including changes in geometry", IABSE, Preliminary Report No.13, pp. 15-22 (1973).

31. Villaverde, R. "Approximate procedure for the seismic nonlinear analysis of nonstructural components in buildings", *J. JSEE.*, **7**(1), pp. 9-24 (2005).


## Appendix

The appendix presents the maximum O.O.P seismic design forces obtained using analytical method, the ones from the ASCE 7-10, and the seismic force modification factors. The values for 3-story and 5-story models are shown in Tables A.1. and A.2. respectively.

**Table A.1.** Maximum O.O.P seismic design forces in 3-story models (kN).

| Models | Analytical | ASCE 7-10 [17] | Ω |
|---|---|---|---|
| $S_3W_3F_1E_{2.5}$ | 9.53 | 6.57 | 1.45 |
| $S_3W_3F_2E_{2.5}$ | 12.60 | 7.01 | 1.80 |
| $S_3W_3F_3E_{2.5}$ | 10.64 | 9.33 | 1.14 |
| $S_3W_3F_1E_{6.5}$ | 9.50 | 6.57 | 1.45 |
| $S_3W_3F_2E_{6.5}$ | 12.39 | 7.01 | 1.77 |
| $S_3W_3F_3E_{6.5}$ | 10.56 | 9.33 | 1.13 |
| $S_3W_3F_1E_{9.5}$ | 9.61 | 6.57 | 1.46 |
| $S_3W_3F_2E_{9.5}$ | 13.00 | 7.01 | 1.85 |
| $S_3W_3F_3E_{9.5}$ | 10.76 | 9.33 | 1.15 |
| $S_3W_4F_1E_{2.5}$ | 14.42 | 9.61 | 1.50 |
| $S_3W_4F_2E_{2.5}$ | 18.34 | 10.25 | 1.79 |
| $S_3W_4F_3E_{2.5}$ | 14.77 | 13.63 | 1.08 |
| $S_3W_4F_1E_{6.5}$ | 14.38 | 9.61 | 1.50 |
| $S_3W_4F_2E_{6.5}$ | 18.12 | 10.25 | 1.77 |
| $S_3W_4F_3E_{6.5}$ | 14.71 | 13.63 | 1.08 |
| $S_3W_4F_1E_{9.5}$ | 14.53 | 9.61 | 1.51 |
| $S_3W_4F_2E_{9.5}$ | 18.00 | 10.25 | 1.76 |
| $S_3W_4F_3E_{9.5}$ | 14.92 | 13.63 | 1.09 |
| $S_3W_5F_1E_{2.5}$ | 19.14 | 12.14 | 1.58 |
| $S_3W_5F_2E_{2.5}$ | 21.66 | 12.94 | 1.67 |
| $S_3W_5F_3E_{2.5}$ | 18.72 | 17.22 | 1.09 |
| $S_3W_5F_1E_{6.5}$ | 19.10 | 12.14 | 1.57 |
| $S_3W_5F_2E_{6.5}$ | 21.25 | 12.94 | 1.64 |
| $S_3W_5F_3E_{6.5}$ | 18.55 | 17.22 | 1.08 |
| $S_3W_5F_1E_{9.5}$ | 19.31 | 12.14 | 1.59 |
| $S_3W_5F_2E_{9.5}$ | 22.37 | 12.94 | 1.73 |
| $S_3W_5F_3E_{9.5}$ | 15.54 | 17.22 | 0.90 |

**Table A.2.** Maximum O.O.P seismic design forces in 5-story models (kN).

| Models | Analytical | ASCE 7-10 [17] | Ω |
|---|---|---|---|
| $S_5W_3F_1E_{2.5}$ | 7.60 | 6.57 | 1.16 |
| $S_5W_3F_2E_{2.5}$ | 11.03 | 6.57 | 1.68 |
| $S_5W_3F_3E_{2.5}$ | 11.31 | 7.01 | 1.61 |
| $S_5W_3F_4E_{2.5}$ | 10.47 | 8.41 | 1.24 |
| $S_5W_3F_5E_{2.5}$ | 9.46 | 9.82 | 0.96 |
| $S_5W_3F_1E_{6.5}$ | 7.70 | 6.57 | 1.17 |
| $S_5W_3F_2E_{6.5}$ | 11.04 | 6.57 | 1.68 |
| $S_5W_3F_3E_{6.5}$ | 11.06 | 7.01 | 1.58 |
| $S_5W_3F_4E_{6.5}$ | 10.19 | 8.41 | 1.21 |
| $S_5W_3F_5E_{6.5}$ | 9.18 | 9.82 | 0.93 |
| $S_5W_3F_1E_{9.5}$ | 7.66 | 6.57 | 1.17 |
| $S_5W_3F_2E_{9.5}$ | 11.37 | 6.57 | 1.73 |
| $S_5W_3F_3E_{9.5}$ | 12.21 | 7.01 | 1.74 |
| $S_5W_3F_4E_{9.5}$ | 10.71 | 8.41 | 1.27 |
| $S_5W_3F_5E_{9.5}$ | 9.53 | 9.82 | 0.97 |
| $S_5W_4F_1E_{2.5}$ | 10.38 | 9.61 | 1.08 |
| $S_5W_4F_2E_{2.5}$ | 16.54 | 9.61 | 1.72 |
| $S_5W_4F_3E_{2.5}$ | 16.82 | 10.25 | 1.64 |
| $S_5W_4F_4E_{2.5}$ | 15.16 | 12.30 | 1.23 |
| $S_5W_4F_5E_{2.5}$ | 13.01 | 14.35 | 0.91 |
| $S_5W_4F_1E_{6.5}$ | 10.39 | 9.61 | 1.08 |
| $S_5W_4F_2E_{6.5}$ | 16.18 | 9.61 | 1.68 |
| $S_5W_4F_3E_{6.5}$ | 16.49 | 10.25 | 1.61 |
| $S_5W_4F_4E_{6.5}$ | 14.87 | 12.30 | 1.21 |
| $S_5W_4F_5E_{6.5}$ | 13.41 | 14.35 | 0.93 |
| $S_5W_4F_1E_{9.5}$ | 10.44 | 9.61 | 1.09 |
| $S_5W_4F_2E_{9.5}$ | 16.80 | 9.61 | 1.75 |
| $S_5W_4F_3E_{9.5}$ | 17.34 | 10.25 | 1.69 |
| $S_5W_4F_4E_{9.5}$ | 15.56 | 12.30 | 1.26 |
| $S_5W_4F_5E_{9.5}$ | 13.03 | 14.35 | 0.91 |
| $S_5W_5F_1E_{2.5}$ | 13.85 | 12.14 | 1.14 |
| $S_5W_5F_2E_{2.5}$ | 20.55 | 12.14 | 1.69 |
| $S_5W_5F_3E_{2.5}$ | 22.13 | 12.94 | 1.71 |

**Table A.2.** Maximum O.O.P seismic design forces in 5-story models (kN) (continued).

| **Models** | **Analytical** | **ASCE 7-10 [17]** | **$\Omega$** |
|---|---|---|---|
| $S_5W_5F_4E_{2.5}$ | 19.15 | 15.53 | 1.23 |
| $S_5W_5F_5E_{2.5}$ | 16.69 | 18.12 | 0.92 |
| $S_5W_5F_1E_{6.5}$ | 13.90 | 12.14 | 1.14 |
| $S_5W_5F_2E_{6.5}$ | 19.52 | 12.14 | 1.61 |
| $S_5W_5F_3E_{6.5}$ | 21.73 | 12.94 | 1.68 |
| $S_5W_5F_4E_{6.5}$ | 18.95 | 15.53 | 1.22 |
| $S_5W_5F_5E_{6.5}$ | 16.72 | 18.12 | 0.92 |
| $S_5W_5F_1E_{9.5}$ | 13.80 | 12.14 | 1.14 |
| $S_5W_5F_2E_{9.5}$ | 20.98 | 12.14 | 1.73 |
| $S_5W_5F_3E_{9.5}$ | 22.61 | 12.94 | 1.75 |
| $S_5W_5F_4E_{9.5}$ | 19.53 | 15.53 | 1.26 |
| $S_5W_5F_5E_{9.5}$ | 16.66 | 18.12 | 0.92 |

## Biographies

**Ali R. Kazerounian** is a PhD Candidate at the Civil Engineering Department of Sharif University of Technology in Kish Island, Iran. He is a faculty member at the Civil Engineering Department of Islamic Azad University, Bushehr, Iran. His research focuses on the behavior of nonstructural components in structures.

**Mohammad T. Kazemi** is an Associate Professor at the Civil Engineering Department of Sharif University of Technology, Tehran, Iran. His research interests include fracture mechanics, inelastic analysis of structures, material modeling, and seismic design of structures.